

CIRCUMSTELLAR ENVELOPES OF OH-IR SOURCES

R.J. Cohen
Nuffield Radio Astronomy Laboratories
Jodrell Bank
Macclesfield
Cheshire SK11 9DL
England

ABSTRACT. This article reviews recent radio observations of maser emission from OH, H₂O and SiO molecules in the circumstellar envelopes of OH-IR sources. The different radio lines require different conditions for their excitation, and each therefore probes different regions in the circumstellar envelope. For some stars radio interferometer maps of several maser lines are now available, and a consistent picture of the envelope structure is beginning to emerge.

1. INTRODUCTION

I will present an observational review of the circumstellar envelopes of OH-IR sources, highlighting the use of radio maser lines to probe their structure. The maser lines of OH, H₂O and SiO which I will discuss are very intense, with brightness temperatures of typically 10^{10} K, and each is emitted from different parts of the circumstellar envelope. The lines can now be studied using radio interferometers (VLA, MERLIN and VLBI) on angular scales from 1 arcsec down to 1 milliarcsec, corresponding to linear scales as small as one astronomical unit. These studies contribute to our understanding of the late stages of stellar evolution (M_* and \dot{M}), the physics of mass loss, the physics of the maser excitation processes, the three-dimensional structure of the circumstellar envelopes, circumstellar chemistry, and the effects of magnetic fields which can be investigated using Zeeman splitting of the OH lines. The OH-IR stars also provide a promising new technique for measuring distances by comparing angular and light-travel diameters. Finally as we heard yesterday from Prof. Habing, the OH-IR stars are a special group of stars which can be identified and studied throughout the Galaxy.

2. BASIC IDEAS ABOUT CIRCUMSTELLAR MASERS

The OH-IR sources are believed to be long-period variable stars near the end of the asymptotic giant branch. Their slow pulsations drive material far enough above the stellar surface that dust grains can condense; and

these are then blown away from the star by radiation pressure, dragging the circumstellar gas with them (Goldreich & Scoville 1976). The mass loss rates are estimated to be $\sim 10^{-5} M_{\odot} \text{ yr}^{-1}$.

For the OH, H₂O and SiO masers the line excitation requirements, and also the shapes of the lines themselves, give clues as to the structure of the circumstellar envelope and the location of the masers within it (e.g. Olmon 1977, Elitzur 1981). The maser lines form a natural sequence of decreasing excitation. The SiO lines at 43, 86 GHz etc. are rotational transitions of vibrationally excited SiO. Lines up to $V=3$ have been observed (Scalise & Lépine 1978). The vibrational states have energy levels corresponding to temperatures of $\sim 2000\text{--}5000\text{K}$, and so appreciable population of these states is only likely close to the star. The H₂O 22 GHz line is produced by a transition between two rotationally excited states ($6_{16}\text{--}5_{23}$) each of which is some $\sim 650\text{K}$ above the ground state. H₂O masers are therefore expected to occur near the star, but not so near as SiO masers. Finally the OH 1.6 GHz lines result from hyperfine splitting of the lambda doublet in the rotational ground state ($^2\pi_{3/2}$). These masers would generally be expected to lie furthest from the star.

The physics of cosmic masers has been reviewed recently by Elitzur (1982). The population inversion can be understood for the case of a two-level maser as a simple problem of rates. The populations are increased by so-called pump processes and decreased by loss processes, each of which can involve radiation, collisions or chemistry. Population inversion can be achieved if the pump or the loss rates for the two levels are unequal. Once inversion has been established the maser provides amplification by stimulated emission. The maser output is limited ultimately by the rate at which inversion occurs, and the maser saturates when the maser transition rate per unit volume approaches the inversion rate per unit volume. The maser can also be quenched when the collision rate dominates the other rates and the level populations thermalize.

3. OH1612 MHz MASERS

The OH1612 MHz masers nicely illustrate the physical principles just outlined. The pumping scheme for these masers is purely radiative, involving absorption of 35 μm photons by OH in the ground state, followed by a radiative cascade down the $^2\pi_{1/2}$ ladder and back to the $^2\pi_{3/2}$ ground state. Elitzur, Goldreich & Scoville (1976) showed that inversion of the 1612 MHz transition will occur provided the final transition to the $^2\pi_{3/2}$ ground state is optically thick. The maser will be quenched for $n_{\text{H}_2} \geq 4 \times 10^5 \text{ cm}^{-3}$. The pumping scheme predicts a specific ratio of four 35 μm photons to one 1612 MHz photon for the case of saturation. Observations by Werner et al. (1980) have verified this. The proportionality between 35 μm emission and 1612 MHz emission was observed from source to source, and for each source individually as it varied throughout the stellar cycle. Monitoring of the OH 1612 MHz masers thus enables a purely radio determination of the stellar period to be made (Harvey et al. 1974; Herman 1983).

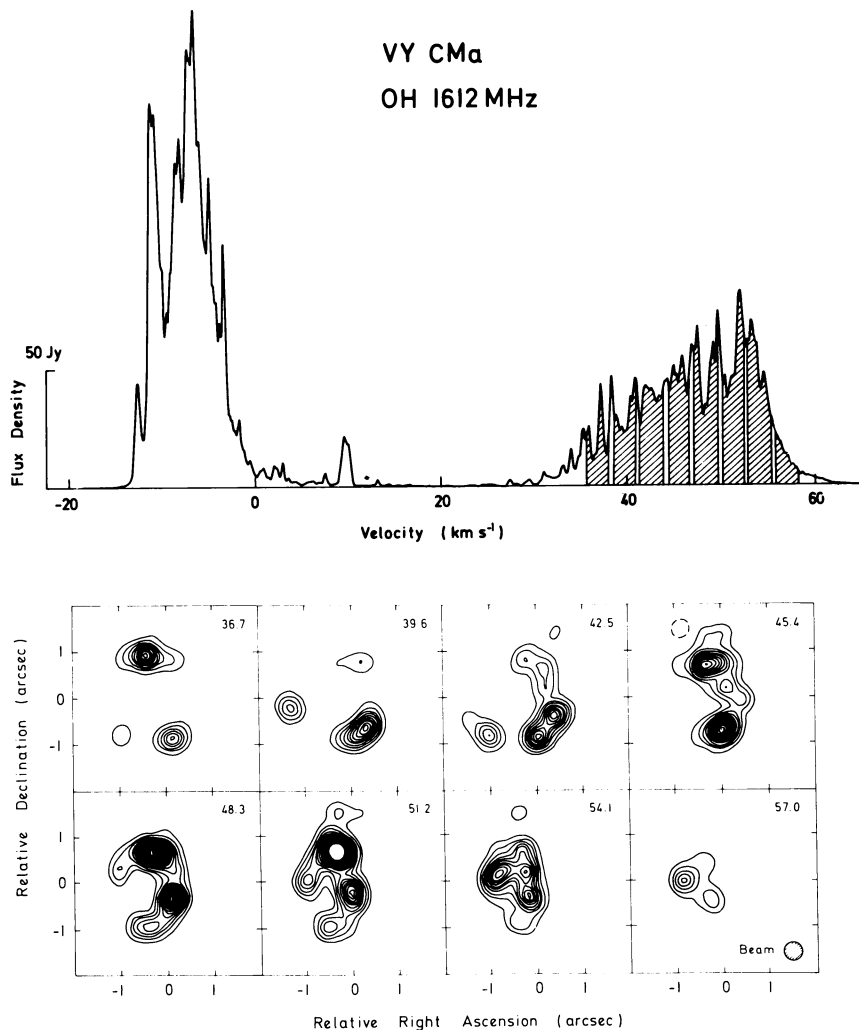


Fig.1. The OH 1612 MHz spectrum of VY CMa shows two main peaks of emission separated by some 50 km s^{-1} . Much fine structure is also evident at the 0.06 km s^{-1} resolution employed here. MERLIN maps of the emission over different velocity ranges (shaded) show different slices through the expanding envelope.

The OH 1612 MHz lines are almost without exception twin-peaked. In the classical OH-IR sources such as IRC10011 the emission varies smoothly with velocity. In other sources such as VY CMA there is much fine structure in the emission profile, as shown in Fig.1. The two emission peaks come from the near and far sides of the expanding circumstellar envelope, where the longest velocity-coherent paths for maser amplification will be found if the outflowing gas has reached terminal velocity (Olnon 1977; Reid et al. 1977). Radio maps made with MERLIN and the VLA confirm that in most cases the 1612 MHz masers are distributed in a uniformly expanding thin shell (Booth et al. 1981; Bowers et al. 1983; Diamond et al. 1985). MERLIN maps of VY CMA are shown in Fig.1. (Perry, unpublished). In this and in most other sources we do not see complete shells of masers. Considering the special excitation requirements and the effects of turbulence on the velocity-coherent paths for maser amplification the lack of complete maser shells is not surprising. Maps of the emission at different velocities show different slices through the maser envelope with the velocities and angular diameters being related in the way predicted by the simple shell model. Some examples of this relation are shown in Fig.2, where the dashed lines indicate least-squares fits to the data. By model-fitting in this way it is possible to determine the shell radius even in cases where the emission at the central velocity (which would show the full shell size) is too weak to be mapped.

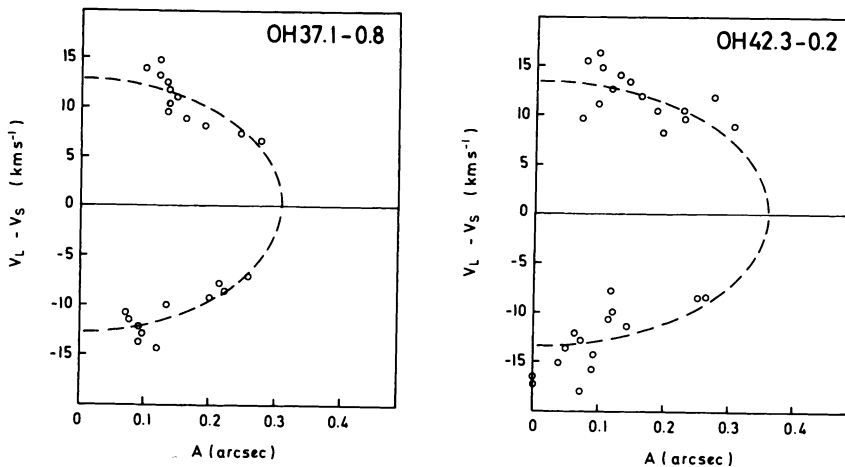


Fig.2 Radial velocities of OH 1612 MHz masers around two OH-IR sources measured relative to the stellar velocity, are plotted against the angular distance from the estimated stellar position. The dashed lines show best fitting expanding shell models, from which the angular radii and expansion velocities of the circumstellar shells are determined (Chapman 1985).

The 1612 MHz emission is pumped by the pulsating 35 μm radiation field and varies in sympathy with it. Although the variations are synchronized with respect to the central star an outside observer sees a measurable phase-lag between the blue-shifted (near) and red-shifted (far) emission peaks. Accurate monitoring of the 1612 MHz masers thus enables the light travel time across the shell to be measured (Jewell et al. 1980; Herman 1983). The phase-lag measurement of the linear diameter can be combined with an interferometric measurement of the angular diameter of the shell to yield a geometrical estimate of the distance to the star (e.g. Baud 1981). These distance measurements could in principle be made accurate to 5%, and so might be of fundamental importance in helping to determine the galactic distance scale.

Phase-lags can also be measured between emission features at intermediate velocities in the OH spectrum. The uniformly expanding shell model predicts a linear change in phase-lag with velocity across the spectrum, and monitoring of this enables a check to be made on the spherical symmetry or otherwise of the envelope (e.g. Bowers & Morris 1984). By monitoring the variations with an interferometer it might be possible to determine phase-lags for individual regions throughout the envelope and so build up a fully three-dimensional picture of the maser shell. This is an experiment which could be started now if it was felt to be important enough.

The shell distribution of OH 1612 MHz masers reflects a true increase in OH abundance at a particular radius from the central star. The OH is produced by photodissociation of H_2O molecules in the external UV radiation field (Goldreich & Scoville 1976). The radius of maximum OH abundance depends in the mass loss rate from the star, and on the strength of the external UV radiation field (Huggins & Glassgold 1982). The dependence on mass loss rate has been confirmed observationally, but there is as yet no firm evidence for the weaker dependence on the UV radiation field.

4. OH MAINLINE MASERS

The OH mainline emission at 1665 and 1667 MHz also varies throughout the stellar cycle, but the variations are larger and less regular than those at 1612 MHz (Harvey et al. 1974; Fillit et al. 1977). These masers too are thought to be radiatively pumped. Infrared radiation from dust which is hotter than the gas can preferentially excite the upper half of the OH lambda doublet, and this inversion will be preserved in the cascade to the ground state, provided of course that the $^2\pi_{1/2}, J=1/2$ to $^2\pi_{3/2}, J=3/2$ transition is optically thin (Elitzur 1978). Pumping efficiencies of 1% are predicted (Bujarrabal et al. 1980a), and these can be increased by line overlap (Bujarrabal et al. 1980b). OH mainline emission is expected to occur in warm optically thin parts of the circumstellar envelope, as compared with the cool optically thick regions which radiate at 1612 MHz.

Published mainline maps are available for only a small number of sources. They divide naturally into two groups. The first group of sources have a classical twin-peaked mainline spectrum, and the maps

show resolved shell structure with the mainline masers at comparable radii to the 1612 MHz masers. Examples are OH 127.8 (Diamond, Norris & Booth 1985) and IRC 10420 (Bowers 1984). OH 127.8 is particularly interesting as the OH 1667 MHz emission at one velocity occurs at the same position angle as a pronounced gap in the 1612 MHz emission at the same velocity. This must reflect an asymmetry in the envelope structure and the mass loss. IRC 10420 is also interesting in that the mainline emission region is larger than the 1612 MHz region, contrary to the pumping models. The second group of stars has more variable line shapes, with emission right across the velocity range. They frequently have large degrees of circular polarization. MERLIN maps show many unresolved masers distributed over a compact region some 10^{15} cm in extent. Examples of such sources are U Ori (Chapman & Cohen 1985) and VX Sgr (Chapman & Cohen 1986). These masers occur in warmer denser regions of the envelope than have been considered in the mainline pumping models.

5. H₂O MASERS

Circumstellar H₂O masers follow the stellar cycle even more irregularly than do OH mainline masers, showing strong variations in amplitude from cycle to cycle, and variations in the line shape (Schwartz et al. 1974; Cox & Parker 1979). Gómez Balboa & Lépine (1986) have attempted to model the amplitude variations in terms of periodic shock waves propagating into the circumstellar envelopes.

The H₂O maser regions are typically 10^{15} cm in extent, and their structure has been shown to vary on a timescale of a year (Johnston, Spencer & Bowers 1985). The most detailed information is available for the supergiant S Per, which has been studied by trans-Atlantic VLBI (Diamond et al. in press). Two dozen individual maser spots were detected over a region some 300 AU in extent. Individual maser spots were resolved, and the spot sizes measured to be a few AU. The kinematics of the H₂O masers can be interpreted in terms of either an expanding thin shell with turbulence, or an expanding thick shell with acceleration.

The pumping of circumstellar H₂O masers is thought to be set up via collisions. Collisional excitation followed by radiative decay can lead to an overpopulation of the so-called "backbone" rotational levels (de Jong 1973) relative to other levels of comparable energy, and in this way population inversions will be set up for several rotational transitions of the H₂O molecule (Cooke & Elitzur 1985). The inner boundary of the H₂O maser region is determined by collisional quenching. The model predicts that the inner radius r_1 should increase with mass loss rate according to

$$r_1 \propto \dot{M}^{2/3} v^{-1}$$

(Cooke & Elitzur 1985), and hence that the size of the maser region should increase with mass loss rate. The rather sparse data presently available are plotted in Fig.3. A correlation in the predicted sense is evident. However it depends entirely on the difference between the supergiants and the Mira-type variables, and more data are needed to establish the result firmly.

6. SiO MASERS

Circumstellar SiO masers show even more irregularity than H₂O masers in their line shapes, in their cycle-to-cycle variations, and in the

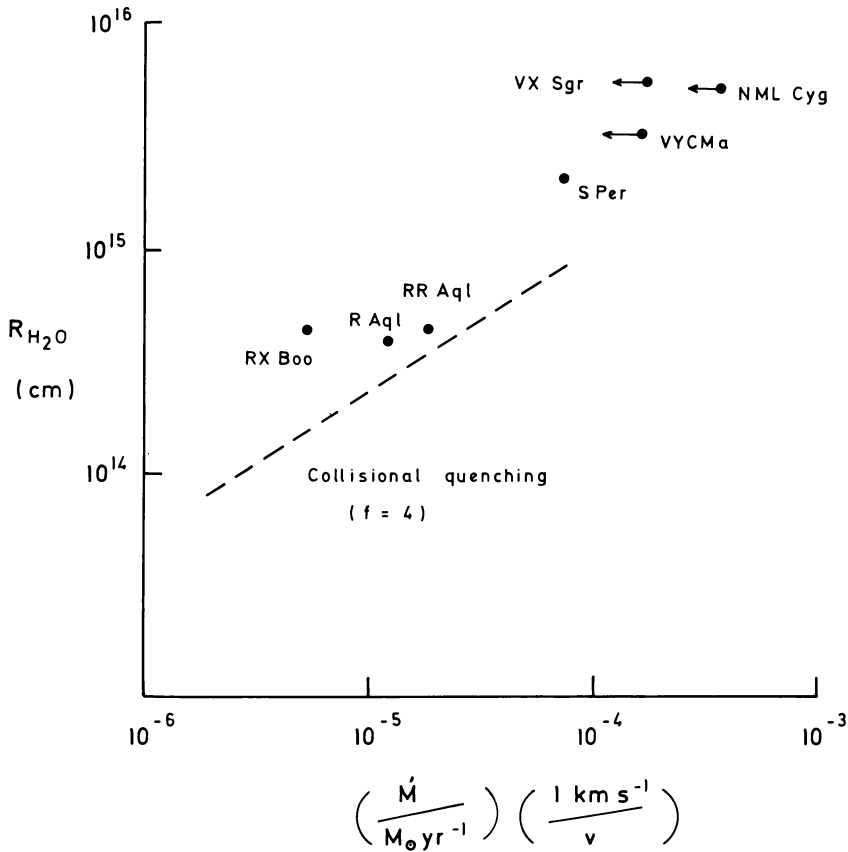


Fig.3. Sizes of circumstellar H₂O maser regions are plotted against mass loss rates for seven stars. The dashed line shows the predicted inner boundary set by collisional quenching of the maser, for an assumed H₂O:H₂ abundance of 4×10^{-4} (Cooke & Elitzur 1985). Sizes of the H₂O maser regions are taken from Johnston, Spencer & Bowers (1985), Cohen & Chapman (1986), Diamond et al. (in press), and unpublished MERLIN data on VY CMa. Mass loss rates are from Gehrz & Wolf (1971) and Bowers, Johnston & Spencer (1983). Mass loss for the supergiants VY CMa, VX Sgr and NML Cyg are shown as upper limits because of asymmetries in the circumstellar envelopes.

variations from star to star. Correlations between SiO maser intensity and stellar light have been seen in most but not all of the sources studied to date (e.g. Lane 1982; Nyman & Olofsson 1986). These correlations do not in themselves constitute proof that the pumping is radiative, since the SiO masers are believed to lie close to the star in hot dense regions where the thermal time constants are very small compared to the stellar period. Theoretical considerations suggest that collisional pumping is most likely (Elitzur 1982). The $J=1-0$ rotational transitions of different vibrationally excited states show strong similarities in their velocity structure. For one star VX Sgr near-simultaneous VLBI maps of the $V=1$ and $V=2$ $J=1-0$ masers have been made. The two lines exhibit strong similarities in their spatial and velocity distributions, which tends to confirm the suggestion that they are generated in the same circumstellar regions despite their different excitations (Lane 1982). The maser region is six stellar radii in extent. Only one other star, R Cas, has been mapped to date, and it shows a distribution of SiO masers some four stellar radii in extent (Lane 1982, and refs therein). This is an area where more observations are urgently needed.

7. VX SGR: A CASE STUDY

The supergiant VX Sgr is the first star for which radio maps of all the classical maser lines are available (Lane 1982; Chapman & Cohen 1986). The data have been combined by Chapman & Cohen, subject to the assumptions given in their paper, to provide a comprehensive radio picture of the circumstellar envelope. A summary of the results is shown in Fig. 4. The SiO, H₂O and OH 1612 MHz masers lie at successively larger distances from the star, as expected from their line excitation requirements. However the OH mainline masers lie at similar distances to the H₂O masers, which seems to indicate some density and/or temperature asymmetries in the envelope structure. Indeed asymmetries and multiple shell structure have been noted in the maser envelopes of most other supergiants studied to date (e.g. Bowers 1984; Diamond et al. 1984).

The kinematics of the masers around VX Sgr are consistent with radial outflow in which the flow velocity increases systematically with distance from the star. The SiO masers show the most irregularity in their velocity pattern, but their kinematics are broadly consistent with expansion (Lane 1982). However the SiO masers are all moving at less than escape velocity. The OH mainline and H₂O masers form a thick shell region in which most of the acceleration appears to take place. By the time the outflowing gas leaves this zone it has achieved escape velocity. Further out the OH 1612 MHz masers are excited in a well-defined thin-shell region. At this stage the outflowing gas is close to terminal velocity. From a more detailed consideration of the velocity field Chapman & Cohen conclude that the driving force per unit mass acting on the outflowing gas must increase outwards to at least fifty stellar radii. An increase in opacity with distance out to twenty stellar radii was in fact incorporated by Goldreich & Scoville (1976) in their model of OH-IR envelopes in order to account for infrared

occultation data (Zappala et al. 1974). It will be interesting to see if observations of other OH-IR sources support this.

An observation relevant to the dynamics and the envelope asymmetries is the strong circular polarization of the OH mainline emission. Cohen & Chapman identify two Zeeman groups in the OH mainline spectra of VX Sgr. The line splitting implies a magnetic field of 2 mG in each case. Such a field has an energy density comparable to that of the outflowing gas, and may therefore be expected to influence the dynamics. In this, as in other respects, it remains to be seen whether VX Sgr is typical of the majority of OH-IR sources.

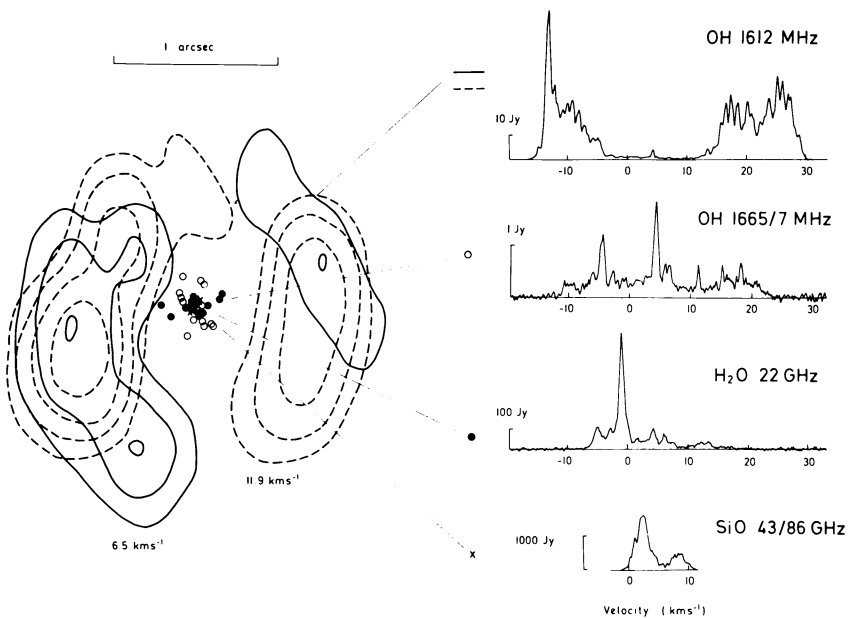


Fig.4 Maser emission from the circumstellar envelope of VX Sgr (from Chapman & Cohen 1986). Spectra of the OH, H₂O and SiO lines are plotted on the right, and the locations of the masers are indicated schematically on the left. For the OH 1612 MHz masers only the emission near the stellar velocity is shown, to make the shell structure clear.

REFERENCES

- Baud, B., 1981. *Astrophys.J.*, 250, L79.
- Booth, R.S., Kus, A.J., Norris, R.P. & Porter, N.D., 1981. *Nature*, 290, 382.
- Bowers, P.F., 1984. *Astrophys.J.*, 279, 350.
- Bowers, P.F., Johnston, K.J. & Spencer, J.H., 1983. *Astrophys.J.*, 274, 733.
- Bowers, P.F. & Morris, M., 1984. *Astrophys.J.*, 276, 646.
- Bujarrabal, V., Destombes, J.L., Guibert, J., Marlière-Demuynck, C., Nguyen-Q-Rieu & Omont, A., 1980a. *Astr.Astrophys.*, 81, 1.
- Bujarrabal, V., Guibert, J., Nguyen-Q-Rieu & Omont, A., 1980b. *Astr.Astrophys.*, 84, 311.
- Chapman, J.M., 1985. Ph.D. Thesis, University of Manchester.
- Chapman, J.M. & Cohen, R.J., 1985. *Mon.Not.R.astr.Soc.*, 212, 375.
- Chapman, J.M. & Cohen, R.J., 1986. *Mon.Not.R.astr.Soc.*, 220, 513.
- Cooke, B. & Elitzur, M., 1985. *Astrophys.J.*, 295, 175.
- Cox, G.C. & Parker, E.A., 1979. *Mon.Not.R.astr.Soc.*, 186, 197.
- Diamond, P.J., Norris, R.P. & Booth, R.S., 1984. *Mon.Not.R.astr.Soc.* 207, 611.
- Diamond, P.J., Norris, R.P. & Booth, R.S., 1985. *Mon.Not.R.astr.Soc.*, 216, 1P.
- Diamond, P.J., Norris, R.P., Rowland, P.R., Booth, R.S. & Nyman, L-A., 1985. *Mon.Not.R.astr.Soc.*, 212, 1.
- Elitzur, M., 1978. *Astr.Astrophys.*, 62, 305.
- Elitzur, M., 1981. "Physical Processes in Red Giants", p.363, eds. Iben, I. & Renzini, A., Reidel, Dordrecht, Holland.
- Elitzur, M., 1982. *Rev.Mod.Phys.*, 54, 1225.
- Elitzur, M., Goldreich, P. & Scoville, N., 1976. *Astrophys.J.*, 205, 384.
- Fillit, R., Proust, D. & Lépine, J.R.D., 1977. *Astr.Astrophys.*, 58, 281.
- Gehrz, R.D. & Woolf, N.J., 1971. *Astrophys.J.*, 165, 285.
- Goldreich, P. & Scoville, N., 1976. *Astrophys.J.*, 205, 144.
- Gómez Balboa, A.M. & Lépine, J.R.D., 1986. *Astr.Astrophys.*, 159, 166.
- Harvey, P.M., Bechis, K.P., Wilson, W.J. & Ball, J.A., 1974. *Astrophys.J.Suppl.*, 27, 331.
- Herman, J., 1983. Ph.D. thesis, University of Leiden.
- Huggins, P.J. & Glassgold, A.E., 1982. *Astr.J.*, 87, 1828.
- Jewell, P.R., Webber, J.C. & Snyder, L.E., 1980. *Astrophys.J.*, 242, L29.
- Johnston, K.J., Spencer, J.H. & Bowers, P.F., 1985. *Astrophys.J.*, 290, 660.
- de Jong, T. 1973. *Astr.Astrophys.*, 26, 297.
- Lane, A.P., 1982. Ph.D. Thesis, University of Massachusetts.
- Nyman, L-A. & Olofsson, H., 1986. *Astr.Astrophys.*, 158, 67.
- Olson, F.M., 1977. Ph.D. Thesis, University of Leiden.
- Reid, M.J., Muhleman, D.O., Moran, J., Johnston, K.J. & Schwartz, P.R., 1977. *Astrophys.J.*, 214, 60.
- Scalise, E. & Lépine, J.R.D., 1978. *Astr.Astrophys.*, 65, L7.
- Schwartz, P.R., Harvey, P.M. & Barrett, A.H., 1974. *Astrophys.J.*, 187, 491.
- Werner, M.W., Beckwith, S., Gatley, I., Sellgren, K., Berriman, G. & Whiting, D.L., 1980. *Astrophys.J.*, 239, 540.

Zappala, R.R., Becklin, E.E., Mathews, K. & Neugebauer, G., 1974.
Astrophys.J., 192, 109.